



## Exploring the effects of a new lifter design and ball mill speed on grinding performance and particle behaviour: A comparative analysis

Ali Safa, Sahraoui Aissat\* 

Research Laboratory for Industrial Technologies, Department of Mechanical Engineering, Faculty of Applied Sciences, Ibn Khaldoun University, Tiaret, Algeria.

\*Corresponding author Email: [sahraoui.aissat@univ-tiaret.dz](mailto:sahraoui.aissat@univ-tiaret.dz)

### HIGHLIGHTS

- The helical lifters considerably increase the grinding efficiency of a ball mill by reducing the wear rate of the lifters and liners.
- The DEM simulation provides qualitative validation of the particle behaviour.
- The power consumed by the mill shows lower values for the new helical lifters.
- The torque reaches its maximum at a rotation rate between 70% and 75%, similar to experimental results.
- For helical lifters, the average kinetic energy rises as the pitch increases.

### ARTICLE INFO

**Handling editor:** Sattar Aljabair

**Keywords:**

Ball mill; helical lifter; grinding performance; particle behavior; discrete element method (DEM).

### ABSTRACT

Ball mills are the leading grinding equipment in the mineral processing industry. Balls are the primary component in the grinding of materials. Lifters lift these balls to the shoulder position before cataracts them to the toe position. Almost all classical theories do not consider the lifter's geometry in calculating the energy consumption of ball mills and focus only on the fill level of the charge, the lifter dimensions, their number, and the mill's rotational speed. To improve the ball mill's performance, a new shape of the lifters was proposed in the present research work. Simulation through the EDEM software and the discrete element method (DEM) was used to predict the particle behaviour and conduct a comparative study on the influence of the lifter geometry and ball mill rotational speed on torque, power draw, and kinetic energy. The validation of our results is evaluated by a confrontation of the experimental tests of discontinuous grinding with a 573 x 160 cm of Bian. The results show that using helical lifters has a more significant effect on the grinding efficiency, the torque, and the power draw of the ball mill. They decrease the wear rate of liners and lifters when mill speeds are extremely high (90%, 100%).

## 1. Introduction

Ball mills are the most common type of fine grinding equipment. They are used in the chemical and pharmaceutical industries and the mineral processing industries to produce cement [1]. These mills consume enormous amounts of electrical energy (50–60%); consequently, comminution costs roughly 60% of the overall investment in a beneficiation plant [2, 3]. As a result, calculating power (or energy) is one of the essential factors in estimating operating costs and determining the best operating conditions for ball mills [4]. Various operational parameters, such as mill speed, the ball charge composition, charge filling, lifter type, and lifter number, significantly impact ball milling grinding efficiency [3]. The grinding efficiency is a function of the quality of the final product, the energy (kWh), and the power (kW), which are used to determine the energy consumption of the mill [4].

EDEM stands for "Event-Driven Execution Model." It is a computational framework used for simulating the behaviour of particulate materials such as powders, granules, and pellets in various industrial processes. The EDEM software uses the Discrete Element Method (DEM) to model the behaviour of individual particles and how they interact with each other and their surroundings. This modelling method can be very beneficial for simulating and understanding the motion of the grinding media of different shapes and sizes in 3D mills [5], where gaining insightful knowledge is challenging due to the phenomena' complexity or the constraints of experimental investigation. Moreover, DEM can show how lifter profiles affect mill power draw and media movement [6].

The number of publications that use the DEM method to study ball mills in depth has increased [7] and has attracted the interest of many researchers. As lifters wear over their service life, this affects the grinding particles' motion and efficiency [8]. Therefore, lifters are changed when their maintenance cost becomes intolerable or when they reach a critical thickness and become susceptible to breaking with continued use [8].

The premature wear of the liners and lifters significantly impacts the annual expenditure of grinding plants [5]. Several studies have been conducted recently for various lifters to examine the forces acting on the lifter bars, the wear of the lifter, the movement of the charge, the torque, and the energy consumption of a ball mill. Here are some examples of what has been done: Using a DEM simulator, Millsoft, Hlungwani et al. [6] investigated the impact of square and trapezoidal lifters on mill power draw and particle flow at various rotational speeds. Djordjevic [9] examined the influence of lifter quality on the power draw of a tumbling mill using the PFC3D code. He concludes that this parameter has a considerable impact and shouldn't be ignored. Makokha et al. [10–12] examine how using cone-lifters affects milling capacity and productivity. Three liner profiles were tested, and an associated numerical simulation was utilized in their studies. A new model of lifter bar wear is proposed by Rezaeizadeh et al. [13] to forecast the life and the evolution of these profiles, to reliably design lifters for a required life and provide a profile that offers optimal overall mill performance over the life of the lifters [13].

Using EDEM software, Powell et al. [3] predicted the lift bars' wear rate and developed a model to update worn lifter profiles gradually. Bian et al. [14] studied the impact of lifter geometry, lifter number, and mill rotational speed on mill performance. In their work, the DEM simulations are compared with the experimental results. Li et al. [15] simulate the particle motion in a ball mill for five distinct lifter shapes at various rotational speeds. They have given rectangular lifters and their impact on the ball mill's working efficiency special consideration. Finally, they adopted the DEM-FEM method [15] to analyze the stress and deformation that lifters go through. This study examines how the ball mill's torque, power consumption, particle behaviour, and kinetic energy are affected by new helical lift bar forms and mill speed through an analysis utilising the three-dimensional discrete element method (3D DEM). Our results are compared with those of Bian's experiments [14].

## 2. Theory and Methodology

### 2.1 Contact Model

The Hertz-Mindlin model is the most commonly used in EDEM simulations [16] among the numerous contact models used to model the contact between particles Figure 1. The model in Figure 1 enables one to calculate forces resulting from particle interaction in normal and tangential directions [16]. Newton's second law can be applied to calculate acceleration. By twice integrating the acceleration, the new particle locations are determined. Using the new positions for each particle, the new contact forces are calculated, and this cycle is repeated for each time step [16,17]. The normal force component is based on the Hertzian contact theory, and the tangential force is based on the work of Mindlin and Deresiewicz [18].

The normal force ( $F_n$ ) is given by Equation 1:

$$F_n = K_n \delta_n + C_n v_n \quad (1)$$

and the tangential force ( $F_t$ ) is given by Equation 2:

$$F_t = \min \{ \mu F_n, K_t \int v_t dt + C_t v_t \} \quad (2)$$

The normal and tangential forces have damping components. The value of the normal damping coefficient is estimated from the coefficient of restitution [18, 19] since the latter is a measure of the energy loss upon collision Equation 3:

$$C_n = -2 \ln e \frac{\sqrt{k_n m^*}}{\sqrt{(\ln e)^2 + \pi^2}} \quad (3)$$

The equivalent mass  $m^*$  is given by Equation 4.

$$m^* = \left( \frac{1}{m_1} + \frac{1}{m_2} \right)^{-1} \quad (4)$$

The particle is subject to a force equal to the sum of normal and tangential contact forces [20]. As indicated in Figure 2a, this force is then decomposed into the x and y directions ( $F_x$  and  $F_y$ , respectively).

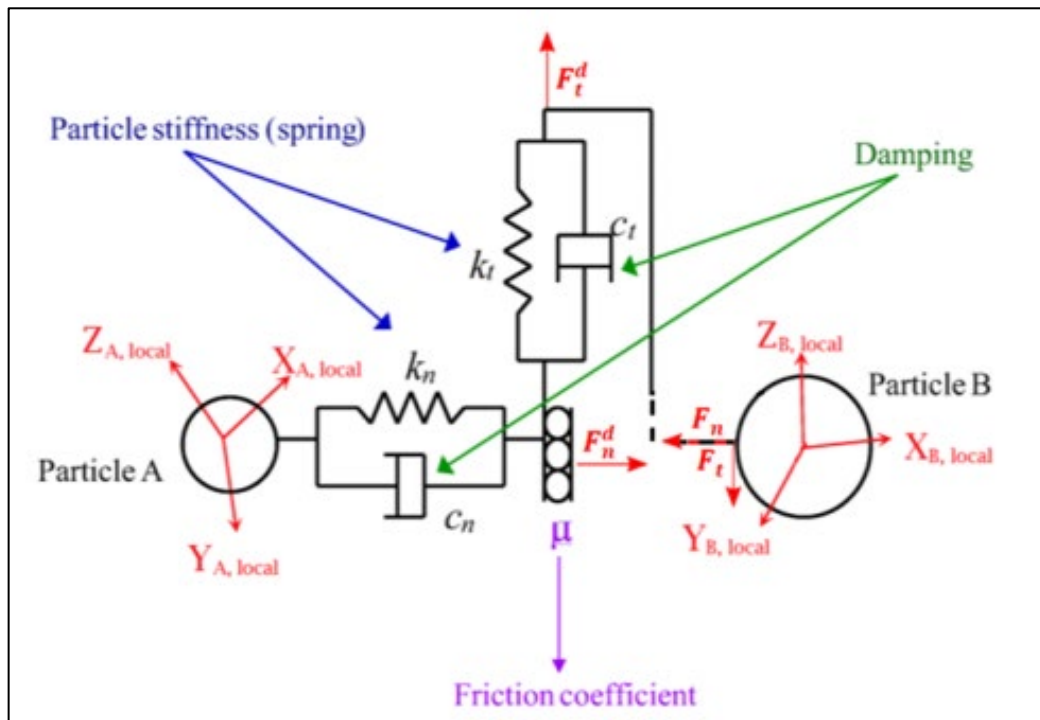


Figure 1: Representation contact model between two particles (Hertz-Mindlin model) [16]

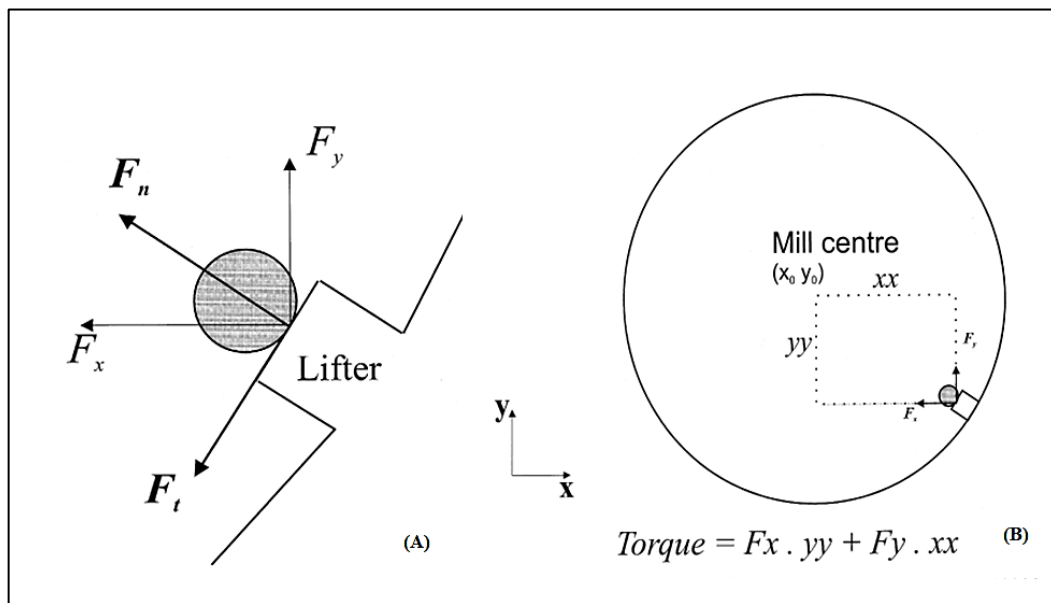


Figure 2: (A) Contact between particle and lifter, (B) DEM torque calculation with \$F\_x\$ and \$F\_y\$ [20]

The DEM code EDEM is used to calculate the torque arm Figure 2b, and the torque is integrated into all contacts and all time steps [20].

The power drawn by the ball mill P (in Watts) is calculated using Equation 5:

$$P = \frac{2\pi NT}{60} \tag{5}$$

With N mill speed in revolutions per minute and T torque (Nm).

### 2.2 Simulation Time

The period between each iteration, or time step [21], must be extremely small ( $< 10^{-6}$  s); it depends on the properties of the material (shear modulus), the number of particles, the shape of the particles, and particle size. Equation 6 was used to calculate the time step based on the Rayleigh time step [21-24]. In our simulation, the time step is set to 20% of the Rayleigh time.

$$dt = T_{\text{step}} < \Delta T_{\text{critical}} = T_{\text{Rayleigh}} = \frac{\pi R \sqrt{\frac{\rho}{G}}}{0,1631\nu+0,8766} \tag{6}$$

With R the particle’s radius, ρ its density, G the shear modulus, and ν the Poisson’s ratio [21].

### 2.3 Lifter Profiles

In our DEM simulations, four lifter profiles (straight and helical with 2, 3, and 4 m pitch) were employed Figures 3a, b, c, and d. Their impacts on torque, power draw, particle motion, and kinetic energy were investigated. Figure 4 depicts the mill's diameter and the dimensions of the trapezoidal lifting bars for the four considered profiles.

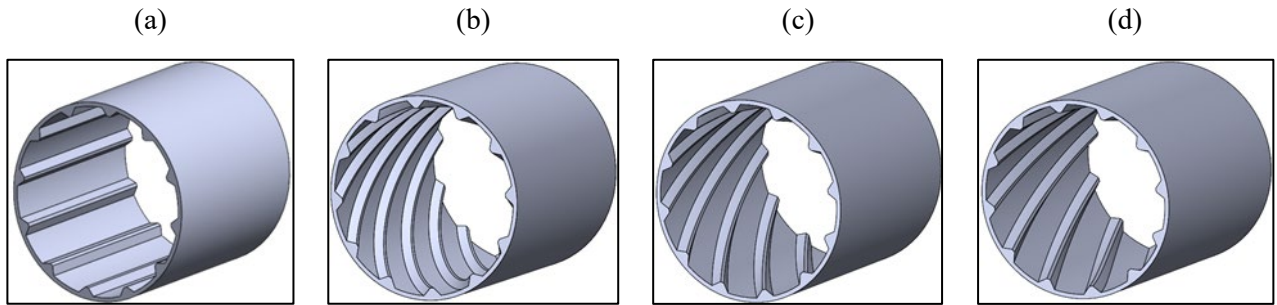


**Figure 3:** 3D geometries of ball mills with (a) straight lifter; (b) helical pitch 2000 (HP2) lifter; (c) Helical pitch 3000 (HP3) lifter; (d) Helical pitch 4000 (HP4) lifter

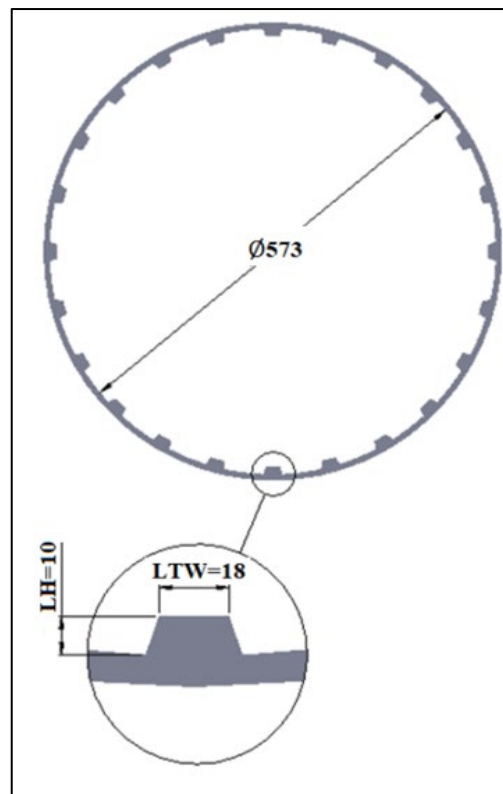


**Figure 4:** Mill’s diameter and the dimensions of the lifter used in the DEM simulation (LH: lifter height (mm); LTW: lifter top width (mm))

### 2.4 Mill Characteristics

The parameters used in this article were selected regarding the work of Bian [14]. The rotational speed varies between 60% and 100% of the critical speed calculated using Equation 7. Other simulation parameters are listed in Table 1.

$$N = \frac{42.3}{\sqrt{D_i}} \text{ (rpm)} \quad (7)$$

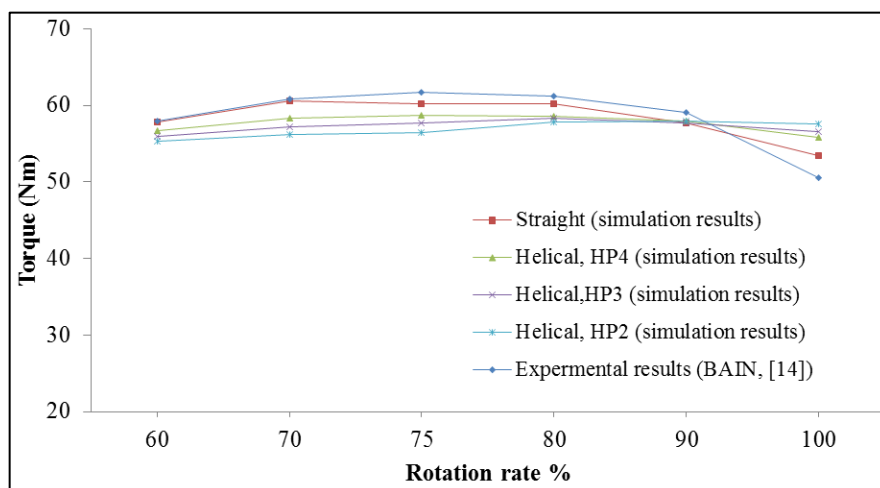
**Table 1:** Ball mill dimensions and load

	Parameters	Values
<b>Ball mill</b>	Internal diameter, mm	573
	Length, mm	160
<b>Lifter</b>	Number of lifters	24
	Dimensions of lifters, mm	10x18
<b>Mill speed</b>	Mill speed, rpm	55,87
	Rotational speed, rpm	(60%, 70%, 75%, 80%, 90%, 100%) x N
<b>Grinding</b>	Mill filling, %	35

### 3. Results and Discussion

#### 3.1 Impact of Rotational Speed and Lifter Shape on Torque and Power Draw

Figures 5 and 6 compare our simulated results using the EDEM software for various rotation speeds and lifter shapes with the experimental data of torque and mill power reported in Bian work [14]. The ball mill fill level is 35%, the lifter height is LH = 10 mm Figure 4, and the lifter bar number is 24. When the rotational speed is altered, DEM simulation and experimental curves are quite close Figure 5. Maximum torque is achieved at a rotational speed between 70% and 80% for straight, HP3, and HP4 lifters. It reaches its maximum at a rotation rate between 70% and 75% for experimental results. The torque decreases slightly until the speed reaches 90%. After this speed, the torque decreases by 6% to 14% compared to the experimental results. For HP2, the torque reaches its maximum at a rotation rate of 90%.

**Figure 5:** Lifter geometry and rotational speed effects on mill torque

The power draw curves are remarkably similar. The values obtained by simulation fit the experimental ones well. Figure 6 shows that the power draw curves continuously increase proportionately to the rotation rate. In our investigation, the mill power consumption reaches its maximum when  $w = 100\%$ . The experimental curves of the power slightly declined when the rotational speed exceeded 90%, and the difference between the experimental curve and the other curves grew. The power consumed by the mill shows lower values for the new helical lifters. This represents a significant advantage in terms of lowering the total cost of energy consumed by mills.

#### 3.2 Impact of Rotational Speed and Lifter Shape on Particles Behaviour

The effect of lifter design on particle behaviour at different rotation rates ( $\omega = 60$  to  $100\%$ ) is examined in Figures 7, 8, and 9. The following simulation parameters were used: lifter number = 24, lifter height LH = 10 mm (Figure 4), and fill level = 35%. The number of high-speed particles and the number of cataracting particles both significantly rise with increasing mill speed for all helical lifters. For HP2, Figures 7a, b, c, and d show that most particles flow cascade, while a few flow cataracts Figures 7e, f. Figures 8a and 9a illustrate a continuous flow of particles in a cascading manner in the case of HP3 and HP4 lifters. As the rotational speed of the mill increases, the intensity of particle movement becomes more pronounced, as depicted in Figures 8b, c, and d for HP3 lifter, and Figures 9b, c, and d for HP4 lifter. In the case of the HP3 and HP4 lifters, the amount of cataracting particles grow significantly at  $\omega = 90\%$  Figures 8e and 9e, nearly covering the mill's whole surface. At 100%, the proportion of projected particles intensifies further and occupies practically the entire mill surface Figures 8f and 9f. Grinding efficiency has improved significantly. For HP3 and HP4, the collisions of particles with liners and lifters are less brutal than in the case of

straight lifters, thereby leading to low wear rates of these liners and lifters. Increased lifter pitch considerably impacts particle behaviour and breaking ability, as shown by Figures 7, 8, and 9.

Figure 10 shows the comparison of particle behaviour between our DEM simulation (Figures 10b, c, d, and e) and the experimental results obtained in the work of Bian [14] Figure 10a. The used parameters are fill level = 35%, lifter height LH = 10 mm Figure 4,  $\omega = 75\%$ , and lifter number = 24. According to Bian's experimental results Figure 10a, flowing particles behave similarly as in the case of the right lifter Figure 10b. When using a low-pitch lifter (HP2), the amount of cataracting particles and the percentage of high-speed particles decrease Figure 10c. The proportion of high-speed particles and the number of cataracting particles in the toe position increases for HP3 Figure 10d and HP4 Figure 10e. Their shoulder position is higher than the HP2 one. In the straight lifter case, many particles come into direct contact with the lifters Figure 10b. This contact significantly accelerates lifter wear rates and reduces lifespan compared to HP3 and HP4 lifters Figures 10d and e.

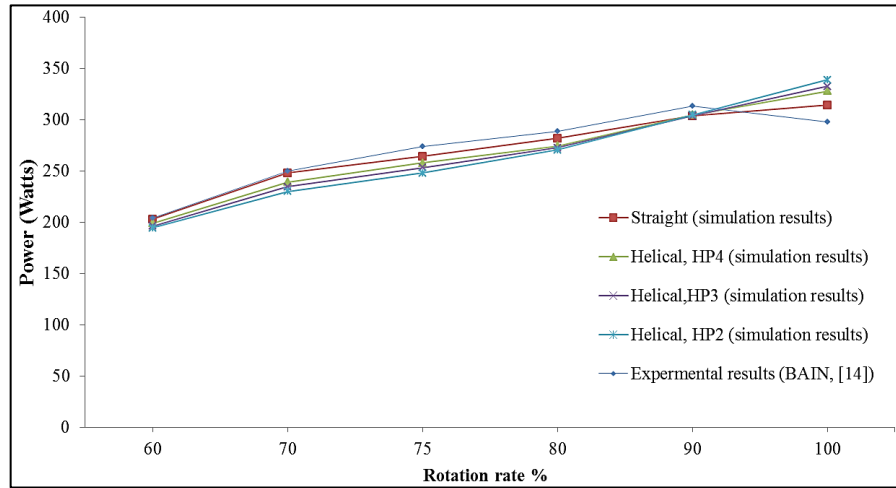


Figure 6: Lifter geometry and rotational speed effects on power draw

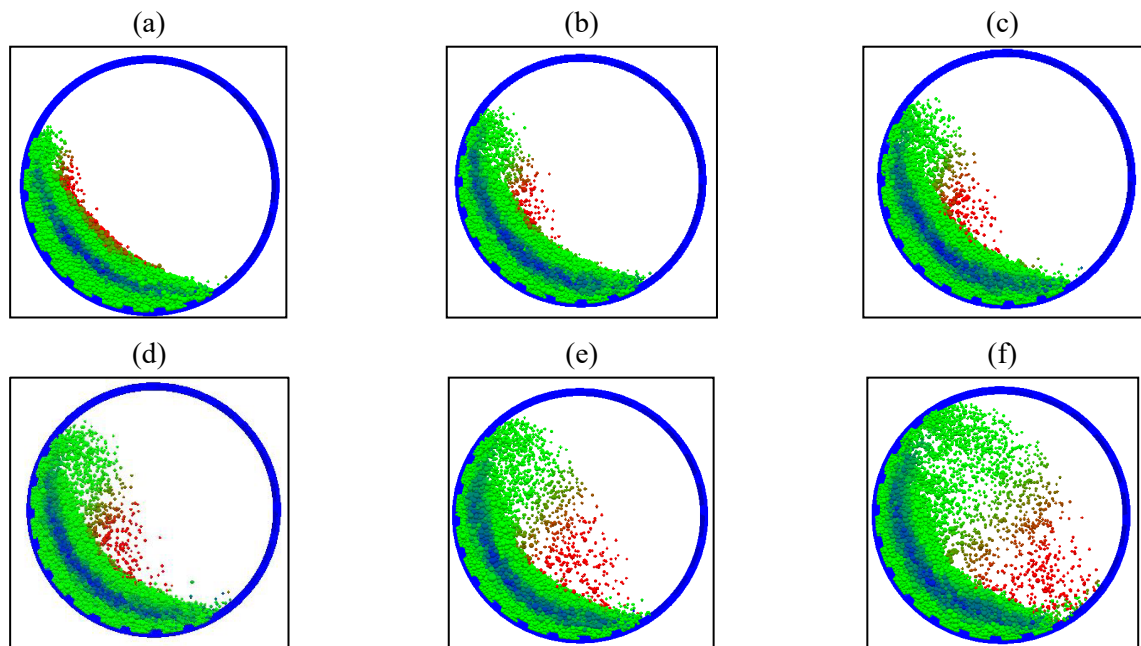


Figure 7: Effect of HP2 lifters on particle behaviour for different rotation rates: (a)  $\omega = 60\%$ ; (b)  $\omega = 70\%$ ; (c)  $\omega = 75\%$ ; (d)  $\omega = 80\%$ ; (e)  $\omega = 90\%$ ; (f)  $\omega = 100\%$



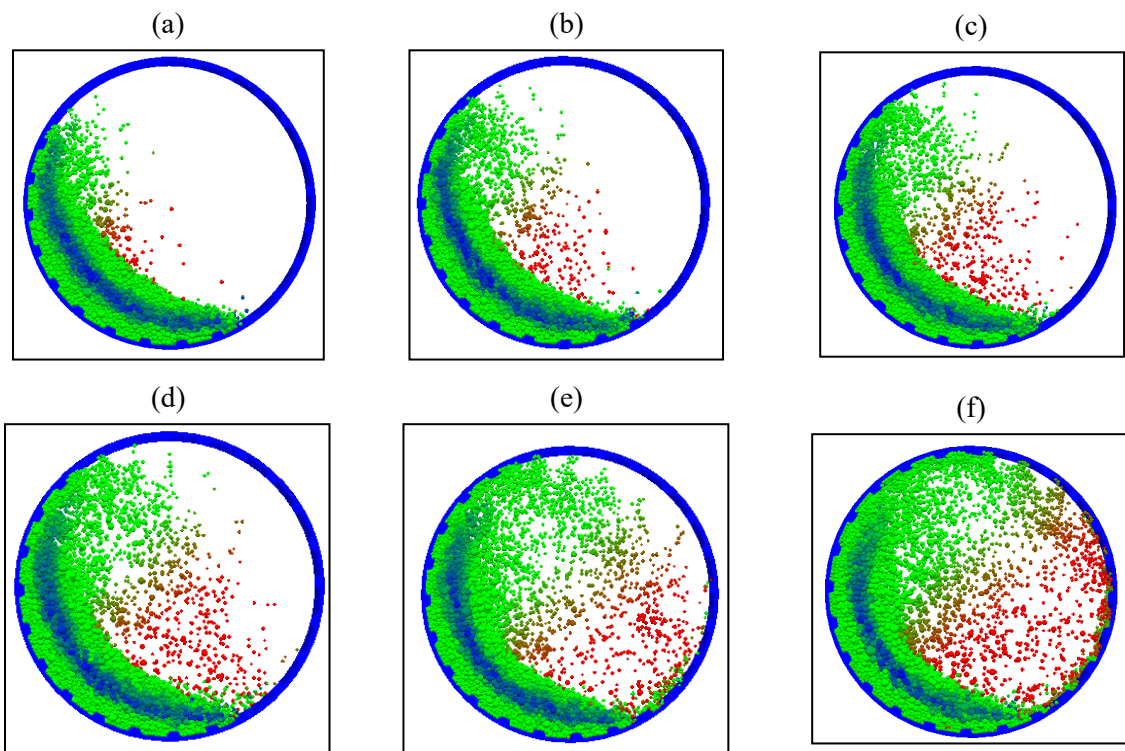


Figure 8: Effect of HP3 lifters on particle behaviour for different rotation rates: (a)  $\omega = 60\%$ ; (b)  $\omega = 70\%$ ; (c)  $\omega = 75\%$ ; (d)  $\omega = 80\%$ ; (e)  $\omega = 90\%$ ; (f)  $\omega = 100\%$

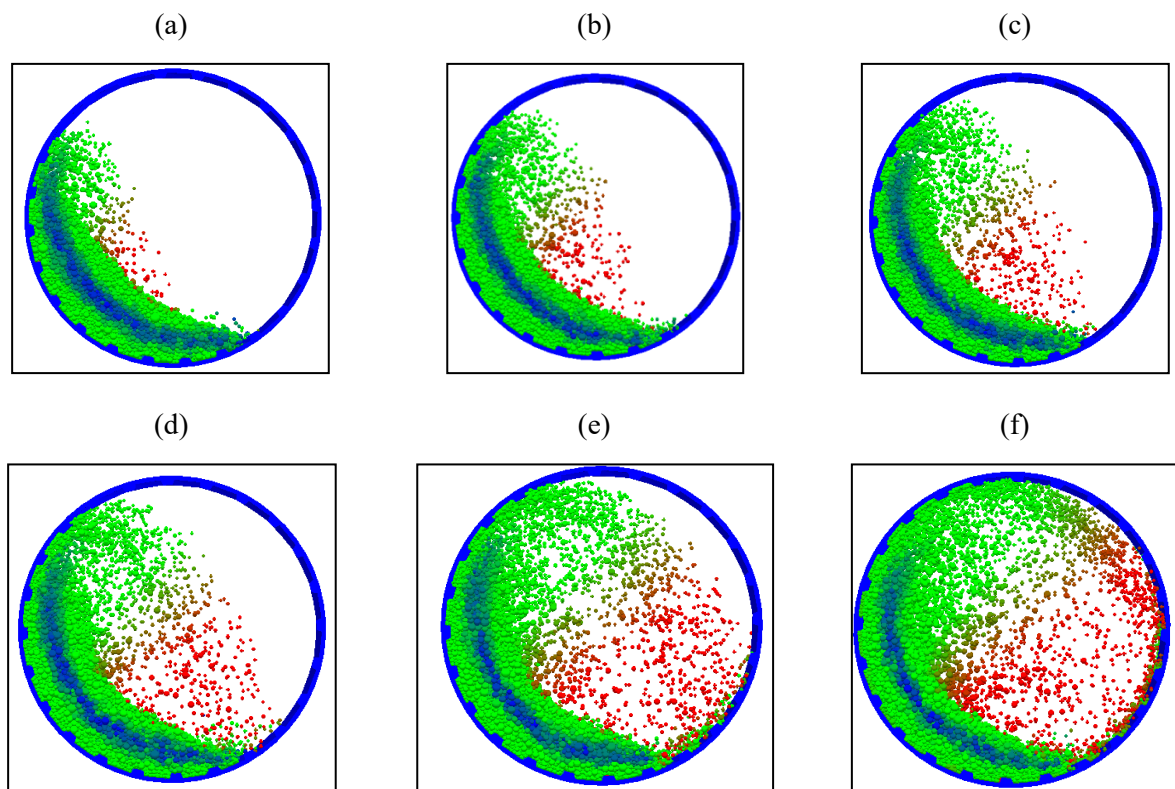


Figure 9: Impact of HP4 lifters on particle behaviour for various rotation rates: (a)  $\omega = 60\%$ ; (b)  $\omega = 70\%$ ; (c)  $\omega = 75\%$ ; (d)  $\omega = 80\%$ ; (e)  $\omega = 90\%$ ; (f)  $\omega = 100\%$

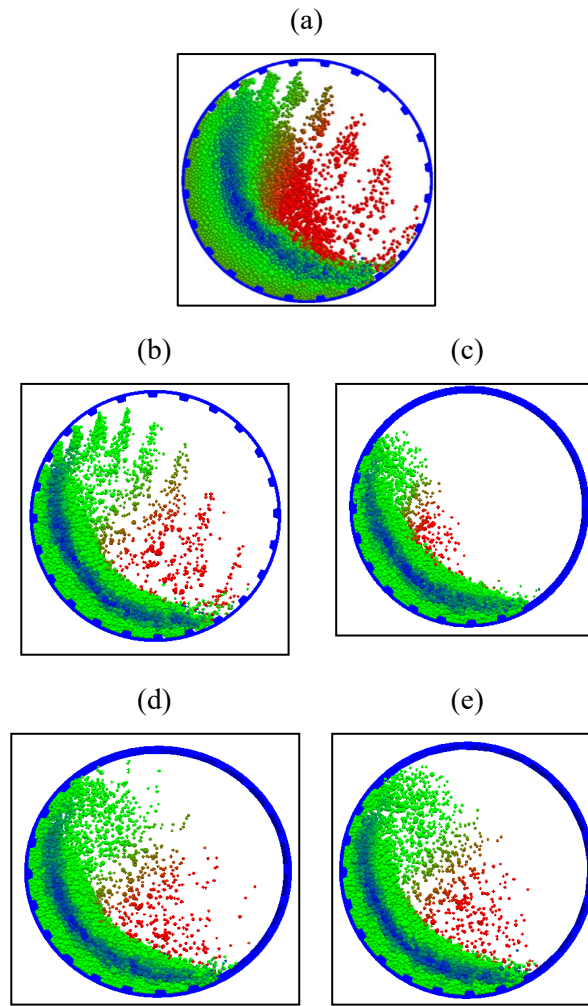


Figure 10: Particles speed diagram for (a) experiment result, Bian [14]; (b) straight lifter; (c) HP2 lifter; (d) HP3 lifter; (e) HP4 lifter

### 3.3 Variation of The Average Kinetic Energy $E_k$ With The Shape of The Lifter and Rotational Speed

The average kinetic energy increases with mill speed. This energy is extremely low for the helical profile of pitch 2000 Figure 11. This result occurs because of the longer contact time of the balls with the mill shell; because they slide longer on the helical profiles before they fall, high-energy collisions cannot effectively occur, which decreases the ball mill's performance. For HP3 and HP4, the average kinetic energy increases, as seen in Figure 11, because a considerable number of particles flow at high speeds, mostly when the mill speeds are high, and they grind efficiently at high energy.

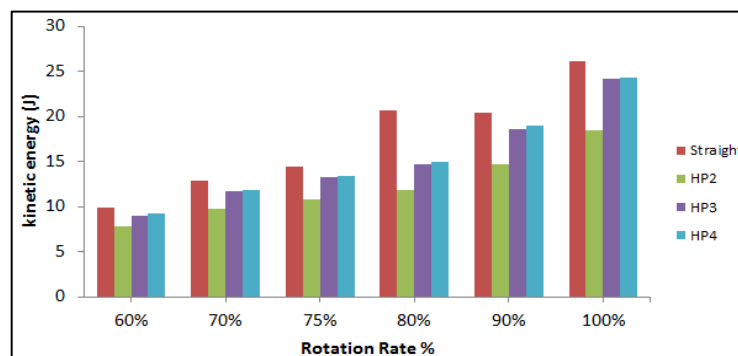


Figure 11: Variation of mean kinetic energy with the shape of lifters and mill speed

## 4. Conclusion

In this work, a new lifter design is proposed. The aim was to compare the torque, power consumption, particle behaviour, and kinetic energy of a ball mill with the experimental results obtained in the work of Bian [14]. Table 2 summarizes the results of this study for  $\omega = 75\%$  and allows drawing the following conclusions:



- 1) In this study, DEM considered an accurate numerical calculation method was employed in this study to estimate mill torque, power consumption, and particle motion.
- 2) The mill speed and lifters geometry have a significant impact on particle behaviour. The DEM simulation used in this study provides qualitative validation of particle behaviour, which is compared with the experimental results obtained in the work of Bian. The results show that more high-speed particles are present when the lifter pitch rises (catacting medium). Therefore, to increase the grinding efficiency and the quality of the end product, the lifter's pitch should be appropriately raised.
- 3) The less violent collisions of the particles projected by HP3 and HP4 lead to low wear rates for liners and lifters.
- 4) The mill torque increases and peaks between 70% and 75%, consistent with Bian's experimental results. It declines after this speed. The simulated values of the helical lifters are lower than the experimental values and represent an average difference of 1.60.
- 5) When the rotational speed increases, helical lifters have little impact on the power draw curves of a mill. The average difference between these values is 3.30.
- 6) The power consumed by the mill shows values lower for the new helical lifters than those of Bian. This represents a significant advantage in terms of lowering the total cost of energy consumed by mills.
- 7) The average kinetic energy is extremely low for the helical profile HP2. For HP3 and HP4, the average kinetic energy increases significantly as rotational speed increases.

**Table 2:** Summary of the results obtained in this work for  $\omega = 75\%$

Lifters	Torque (Nm)	Power (W)	$E_k$ (J)	Particle behaviour	Grinding performance
Straight	60,1655	264,1265	14,5010	Cataract	Increases
Helical, HP2	56,4997	248,0336	10,7853	Cascade	Decreases
Helical, HP3	57,6463	253,0672	13,2627	Cataract	Increases
Helical, HP4	58,7478	257,9028	13,4020	Cataract	Increases
BAIN, [14]	61,7403	273,5096	Not available	Cataract	Increases

## Nomenclature

K	Particle stiffness
C	Dash-pot damping coefficient
v	Relative velocity of the particles
dt	Time step of the simulation
e	Coefficient of restitution
$m^*$	Effective (equivalent) mass
$\delta$	Particle overlap
$\mu$	Coefficient of friction

## Author contributions

Conceptualization, A. Safa and S. Aissat; Methodology, A. Safa and S. Aissat; EDEM software, A. Safa; Analysis and investigation, A. Safa and S. Aissat; bibliographical sources, A. Safa; writing original and review the manuscript, A. Safa and S. Aissat. All authors have read and approved the final published version of the paper.

## Funding

This research work received no external funding from natural or legal persons.

## Data availability statement

The data supporting this study's findings are available on request from the corresponding author.

## Conflicts of interest

The authors declare that there is no conflict of interest.

## References

- [1] I. de Camargo, J. Fiore, P. Lova, R. Erberelia, C.A. Fortulana, Influence of Media Geometry on Wet Grinding of a Planetary Ball Mill, *Mater. Res.*, 22 (2019) 2-6. <https://doi.org/10.1590/1980-5373-MR-2019-0432>
- [2] L. Si, Y. Cao, G. Fan, The Effect of Grinding Media on Mineral Breakage Properties of Magnetite Ores, *Geofluids*, 2021 (2021) 1–9. <https://doi.org/10.1155/2021/1575886>

- [3] G.S. Abdelhaffez, A.A. Ahmed, H.M. Ahmed, Effect of grinding media on the milling efficiency of a ball mill, *Rudarsko-geološko-naftni zbornik*, 37 (2022) 171-177. <https://doi.org/10.17794/rgn.2022.2.14>
- [4] S. Chehrehghani, H.H. Gharehgheshlagh, S. Haghikia, Power consumption management and simulation of optimised operational conditions of ball mills using the Morrell Power model: A case study, *Rudarsko-geološko-naftni zbornik*, 37 (2021) 123-135. <https://doi.org/10.17794/rgn.2022.2.11>
- [5] M.S. Powell, N.S. Weerasekara, S. Cole, R.D. LaRoche, J. Favier, DEM modelling of liner evolution and its influence on grinding rate in ball mills, *Miner. Eng.*, 24 (2011) 341–351. <https://doi.org/10.1016/j.mineng.2010.12.012>
- [6] O. Hlungwani, J. Rikhotso, H. Dong, M.H. Moys, Further validation of DEM modeling of milling: effects of liner profile and mill speed, *Miner. Eng.*, 16 (2003) 993–998. <https://doi.org/10.1016/j.mineng.2003.07.003>
- [7] D. Daraio, J. Villoria, A. Ingram, A. Alexiadis, E. Hugh Stitt, M. Marigo, Validation of a Discrete Element Method (DEM) Model of the Grinding Media Dynamics within an Attritor Mill Using Positron Emission Particle Tracking (PEPT) Measurements, *Appl. Sci.*, 9 (2019) 4816. <https://doi.org/10.3390/app9224816>
- [8] Tshibangu Kalala, J. Discrete element method modeling of forces and wear on mill lifters in dry ball milling. Ph.D. Thesis, University of Witwatersrand, Johannesburg, 2008.
- [9] N. Djordjevic, Discrete element modelling of the influence of lifters on power draw of tumbling mills, *Miner. Eng.*, 16 (2003) 331–336. [https://doi.org/10.1016/S0892-6875\(03\)00019-0](https://doi.org/10.1016/S0892-6875(03)00019-0)
- [10] A.B. Makokha, M.H. Moys, Towards optimising ball-milling capacity: effect of lifter design, *Miner. Eng.*, 19 (2006) 1439–1445. <https://doi.org/10.1016/j.mineng.2006.03.002>
- [11] A.B. Makokha, M.H. Moys, Effect of cone lifters on the discharge capacity of the mill product: case study of a dry laboratory-scale air-swept ball mill, *Miner. Eng.*, 20 (2007) 124–131. <https://doi.org/10.1016/j.mineng.2006.07.010>
- [12] A.B. Makokha, M.H. Moys, M.M. Bwalya and K. Kimera, A new approach to optimising the life and performance of worn liners in ball mills: experimental study and DEM simulation, *Int. J. Miner. Process.*, 84 (2007) 221–227. <https://doi.org/10.1016/j.minpro.2006.09.009>
- [13] M. Rezaeizadeh, M. Fooladi, M.S. Powell, S.H. Mansouri, N.S. Weerasekara, A new predictive model of lifter bar wear in mills, *Miner. Eng.*, 23 (2010) 1174–1181. <https://doi.org/10.1016/j.mineng.2010.07.016>
- [14] X. Bian, G. Wang, H. Wang, S. Wang, W. Lu, Effect of Lifters and Mill Speed on Particle Behaviour, Torque, and Power Consumption of a Tumbling Ball Mill: Experimental Study and DEM Simulation, *Miner. Eng.*, 105 (2017) 22-35. <https://doi.org/10.1016/j.mineng.2016.12.014>
- [15] Z. Li, Y. Wang, W. Lin, K. Li, Studies on the Performance of Ball Mill with Liner Structure Based on DEM, *J. Eng. Technol. Sci.*, 50 (2018) 157-178. <https://doi.org/10.5614/j.eng.technol.sci.2018.50.2.2>
- [16] P. Muhayimana, J.K. Kimotho, M.K. Ndeto, H.M. Ndiritu, Effects of Lifter Configuration on Power Consumption of Small Scale Ball Mill, *J. Sustain. Res. Eng.*, 4 (2018) 171-183.
- [17] S. Kolahi, M. J. Chegeni, K. S. Shabani, Investigation of the effect of industrial ball mill liner type on their comminution mechanism using DEM, *Int. J. Min. Geo-Eng.*, 55 (2021) 97-107. <https://doi.org/10.22059/ijmge.2020.289423.594826>
- [18] T. Yasunaga, M. Yoshida, A. Shimosaka, Y. Shirakawa, T. Andoh, H. Ichikawa, N. Ogawa, H. Yamamoto, Mathematical modelling of coating time in dry particulate coating using mild vibration field with bead media described by DEM simulation, *Adv Powder Technol.*, 33 (2022) 103779. <https://doi.org/10.1016/j.apt.2022.103779>
- [19] P.K. Cleary, P. Owen, Effect of particle shape on structure of the charge and nature of energy utilisation in a SAG mill, *Miner. Eng.*, 132 (2019) 48–68. <https://doi.org/10.1016/j.mineng.2018.12.006>
- [20] M.A. van Nierop, G. Glover, A.L. Hinde, M.H. Moys, A discrete element method investigation of the charge motion and power draw of an experimental two-dimensional mill, *Int. J. Miner. Process.*, 61 (2001) 77–92. [https://doi.org/10.1016/S0301-7516\(00\)00028-4](https://doi.org/10.1016/S0301-7516(00)00028-4)
- [21] EDEM, User Guide; DEM Solut. Ltd. 2017.
- [22] M. Marigo, E.H. Stitt, Discrete element method (DEM) for industrial applications: Comments on calibration and validation for the modelling of cylindrical pellets, *KONA powder part. J.*, (2015) 32 236–252. <https://doi.org/10.14356/kona.2015016>
- [23] S. Rosenkranz, S. Breitung-Faes, A. Kwade, Experimental investigations and modelling of the ball motion in planetary ball mills, *Powder Technol.*, 212 (2011) 224-230. <https://doi.org/10.1016/j.powtec.2011.05.021>
- [24] K. Kyong-Chol, J. Tao, K. Nam-II, K. Cholu, Effects of ball-to-powder diameter ratio and powder particle shape on EDEM simulation in a planetary ball mill, *J. Indian Chem. Soc.*, 99 (2022) 100300. <https://doi.org/10.1016/j.jics.2021.100300>